

Article

# Synthesis of vanadium-containing catalytically active phases for exhaust gas neutralizers of motor vehicles and industrial enterprises

Bolatbek Khussain <sup>1</sup>, Alexandr Brodskiy <sup>1,\*</sup>, Alexandr Sass <sup>1</sup>, Kenzhegul Rakhmetova <sup>1</sup>, Vladimir Yaskevich <sup>1</sup>, Valentina Grigor'eva <sup>1</sup>, Altay Ishmukhamedov <sup>1</sup>, Anatoliy Shapovalov <sup>1</sup>, Irina Shlygina <sup>1</sup>, Svetlana Tungatarova <sup>1,2\*</sup>, Atabek Khussain <sup>1</sup>

<sup>1</sup> D.V. Sokolsky Institute of Fuel, Catalysis and Electrochemistry, 142, Kunaev str., Almaty, 050010, Kazakhstan

<sup>2</sup> al-Farabi Kazakh National University, 71, al-Farabi str., Almaty, 050040 Kazakhstan

\* Correspondence: a.brodskiy@ifce.kz; Tel.: +7-777-706-6713; tungatarova58@mail.ru; Tel.: +7-727-291-6632

**Abstract:** The catalytically active vanadium-containing system on  $\gamma$ -Al<sub>2</sub>O<sub>3</sub> was studied using a wide range of physical and chemical methods depending on the synthesis conditions. It is shown that the vanadium-containing system includes several complexes with different thermal stability and catalytic activity. Low-active complexes are destroyed with the formation of more active ones based on V<sub>2</sub>O<sub>5</sub> oxide as the temperature of heat treatment increases. It can be assumed that the V<sub>2</sub>O<sub>5</sub> oxide has the decisive role in its catalytic activity. It was concluded that the vanadium-containing catalytic system on aluminum oxide, in the studied temperature range, is thermal stable and shows high activity not only in the reduction of nitrogen oxides but also in the oxidation of hydrocarbons (even of the most difficult ones, such as oxidizable methane). These properties of the system make it quite promising in the field of application for purification of exhaust gases of motor transport and industrial enterprises from environmentally harmful components as well as for understanding the mechanism of the action of catalysts in these processes, which is very important for solving the problems of decarbonization and achieving carbon neutrality.

**Keywords:** neutralizers; catalysts; vanadyl sulfate; aluminium oxide; oxidation of saturated hydrocarbons

## 1. Introduction

Environmental protection is one of the most pressing problems. One of the main factors that have a negative impact on the environment are the exhaust gases of industrial enterprises and vehicles, as a variety of gases enter the atmosphere as a result of their functioning. Harmful toxic emissions include unreacted fuel hydrocarbons, CO, NO<sub>x</sub>, sulfur-containing compounds, soot, etc. Catalytic purification can be one of the most effective and rational ways to neutralize as well as recycle components of harmful emissions, in particular, complete catalytic oxidation of organic substances to carbon dioxide and water, sulfur dioxide and reduction of nitrogen oxides.

Often, catalytic systems of aluminium-cobalt, aluminium-cobalt-magnesium and systems using 4 and 5d transition metals of the VIII group are the basis for catalytic converters of toxic exhaust gas components from motor vehicles and industrial plants [1-22]. As a rule, the latter show the best results, and are the most effective.

Vanadium containing oxide catalytically active phases were synthesized to replace expensive components in neutralizers and to approximate the efficiency of such systems to that of systems based on noble metals. The choice of vanadium oxides is due to the fact that catalytic systems based on vanadium (V) oxide as such [23] and supported on various supports with a high specific surface area, for example, oxides of aluminium, silicon, titanium, etc., are known [24-30], which can be used as oxidation catalysts, in particular,

nitrogen oxides, as well as in the selective purification of exhaust gases from internal combustion engines [31-37].

The emission of incompletely burned and unreacted hydrocarbons into the atmosphere is one of the main and intractable problems in relation to non-stationary consumers of hydrocarbon fuel (internal combustion engines of vehicles, mobile power generators, heat guns, etc.). This is due to the frequent switching of the engine operation mode, causing changes in the conditions of hydrocarbon fuel combustion [38].

In this regard, vanadium containing oxide catalytically active phases that exhibit activity in red-ox reactions were synthesized as specified above. Physical and chemical properties and catalytic activity in the oxidation of saturated hydrocarbons using the example of methane, as the most difficult object to be oxidized, were studied by a wide range of physicochemical methods.

## 2. Results and Discussion

Powdered samples of the initial compound  $\text{VO}_2 \cdot 3\text{H}_2\text{O}$  and the catalytically active phase 10%  $\text{V}/\gamma\text{-Al}_2\text{O}_3$  under different temperature conditions were studied using the electron paramagnetic resonance (EPR) method. The samples were calcined for 1 h in air at varying temperatures. The EPR spectra were recorded at room temperature in air in the registration mode: microwave power -2 mW, modulation amplitude 20 gauss, time constant 0.1 s, magnetic field  $3300 \pm 2500$  gauss, field sweep time 2.5 min.

Figure 1 shows EPR spectra of 10%  $\text{V}/\gamma\text{-Al}_2\text{O}_3$  catalyst. Table 1 shows the results of their processing. The  $^{51}\text{V}$  isotope is the only stable isotope with a nucleus spin of 7/2. So its EPR signal should have 8 superfine splitting components with slightly different g-factors. Thus, the recorded total spectrum was the sum of all signal components. Indeed, at least eight poorly resolved and strongly broadened hyperfine structure components are observed in the EPR spectra of the samples (Figure 1).

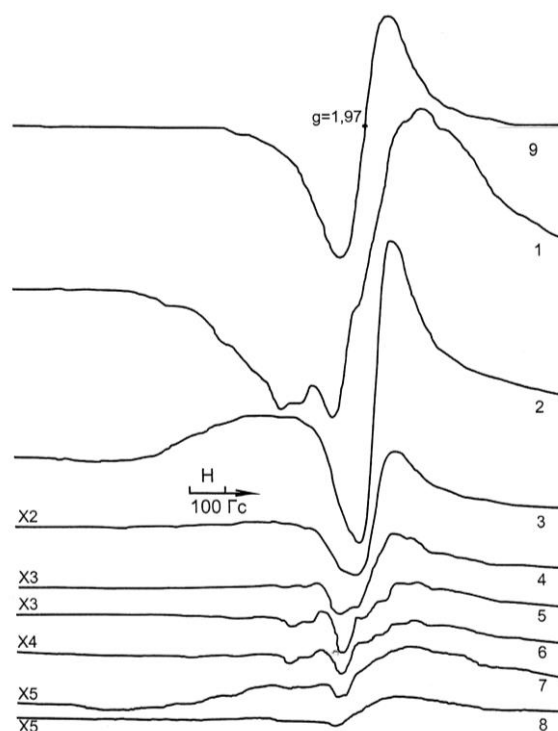


**Figure 1.** EPR spectra of 10%  $\text{V}/\gamma\text{-Al}_2\text{O}_3$ . 1 - initial catalyst after heating in air for 1 h at temperatures: 2 - 300 °C; 3 - 400 °C; 4 - 500 °C; 5 - 600 °C; 6 - 700 °C; 7 - 800 °C; 8 - 900 °C; 9 - initial  $\text{VO}_2 \cdot 3\text{H}_2\text{O}$ .

The EPR spectra have a large  $\Delta H$  width (116 - 483 gauss) and a g-factor  $\approx 1.97$ . The spectra intensity decreases with increase of the sample calcination temperature. The EPR signal is probably related to  $\text{V}^{4+}$  ions included in the vanadyl ion of the initial  $\text{VO}_2 \cdot 3\text{H}_2\text{O}$ .

SO<sub>4</sub>·3H<sub>2</sub>O that undergoes destruction during the interaction of aluminium oxide with the vanadyl sulfate sulfo group when supported on the carrier. The resulting free vanadyl oxide transforms into diamagnetic vanadium oxide V<sub>2</sub>O<sub>5</sub> upon supporting and drying at room temperature. This process increases with increase of the temperature (Table 1).

**Table 1.** Results of EPR spectra of vanadium-containing phases at various heating temperatures.

Sample	Intensity, amplitude (a.u.)	g-factor	ΔH (gauss)
Initial 10% V/γ-Al <sub>2</sub> O <sub>3</sub>	120	1.99	270
300 °C	116	1.97	261
400 °C	24	1.97	116
500 °C	13	1.97	155
600 °C	11	1.97	193
700 °C	6.5	1.97	213
800 °C	1.3	1.97	213
900 °C	1.5	1.97	174
VOSO <sub>4</sub> ·3H <sub>2</sub> O	2,250	1.97	126

Since 10% vanadium in terms of metal is present on the carrier, the signal amplitude intensity for all supported samples should be increased 10-fold, and it will increase from 2250 to 9570 for VOSO<sub>4</sub>·3H<sub>2</sub>O in terms of metallic vanadium (Table 2).

Consequently, even a simple impregnation of γ-Al<sub>2</sub>O<sub>3</sub> with an aqueous solution of vanadyl sulfate and drying at room temperature results in a decrease in the signal amplitude from V<sup>4+</sup> ions from 9,570 to 1,200 a.u. or almost 8 times that can be associated with the formation of V<sub>2</sub>O<sub>5</sub> diamagnetic phase.

The elemental composition of powdered samples of catalytically active phase 10% V/γAl<sub>2</sub>O<sub>3</sub> and after its calcination was investigated with energy dispersive X-ray fluorescence spectroscopy. The results are shown in Table 2.

**Table 2.** Elemental content in 10% V/γAl<sub>2</sub>O<sub>3</sub> calcined in air at different temperatures.

T (°C)	Elements (wt%)					Total
	O	Al	Si	S	V	
25 (initial)	45.07	40.60	0.42	5.19	8.72	100
300 °C	44.79	41.62	0.11	5.11	8.37	100
400 °C	45.28	41.30	0.07	4.95	8.40	100
500 °C	47.23	41.16	0.09	4.04	7.49	100
600 °C	45.69	44.14	0.10	3.21	6.86	100
700 °C	37.92	50.99	0.08	0.00	11.01	100
800 °C	40.42	48.78	0.08	0.00	10.72	100

As follows from Table 2, an increase in the calcination temperature results in the disappearance of sulfur that is associated with the formation of V<sub>2</sub>O<sub>5</sub> vanadium oxide from VOSO<sub>4</sub>·3H<sub>2</sub>O and decomposition of aluminum sulfate.

A diffractogram of the 10% V/Al<sub>2</sub>O<sub>3</sub> initial sample dried in air at room temperature is shown in Figure 2. There are three main peaks corresponding to V<sub>2</sub>O<sub>5</sub> (4.37; 3.40; 2.87; ASTM 9-387) in the background of broad peaks corresponding to alumina. The same pattern persists after heating the samples up to 400 °C (Figure 3).

Diffraction maxima from Al<sub>2</sub>(SO<sub>4</sub>)<sub>3</sub> (5.86; 3.51-3.52; 2.03; ASTM 30-43) additionally appear in the samples heated at temperatures above 400 °C (Figure 4). The diffraction maxima from aluminium sulfate disappear at heating temperatures of 700 °C and above, and the intensity of the maxima of V<sub>2</sub>O<sub>5</sub> oxide increases (Figure 5).

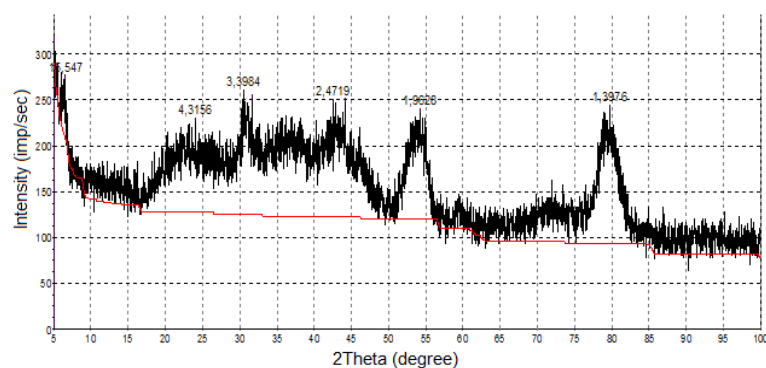


**Figure 2.** Diffractogram of 10% V/Al<sub>2</sub>O<sub>3</sub> catalyst (initial).

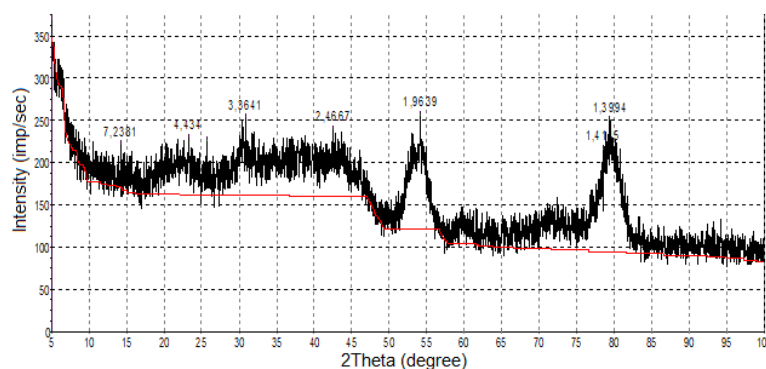


**Figure 3.** Diffractogram of 10% V/Al<sub>2</sub>O<sub>3</sub> catalyst (400 °C).

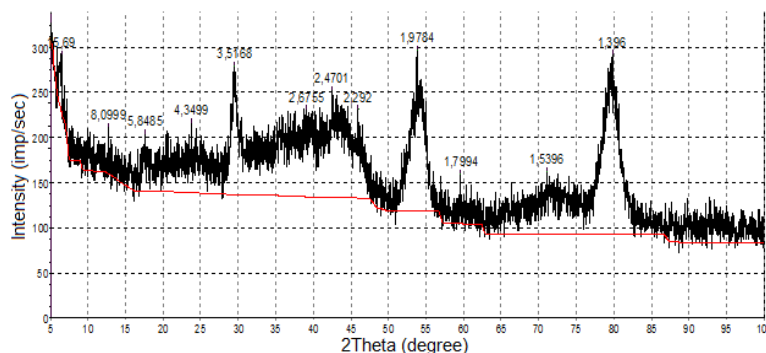


**Figure 4.** Diffractogram of 10% V/Al<sub>2</sub>O<sub>3</sub> catalysts (600 °C).

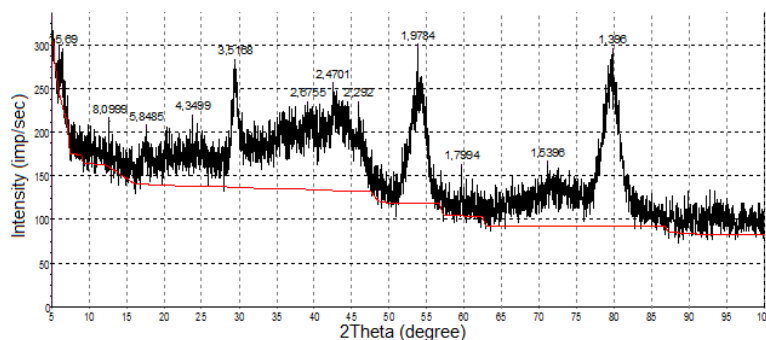


**Figure 5.** Diffractogram of 10% V/Al<sub>2</sub>O<sub>3</sub> catalysts (700 °C).

The narrowing of the diffraction peaks (Figure 5) is associated with a better oxidation of the sample and, as a consequence, the reduction of the X-ray amorphous component.

The data obtained by scanning electron microscopy also testify to the change in surface morphology of the 10% V/Al<sub>2</sub>O<sub>3</sub> system in the transition from 500 to 700 °C (Fig-

ure 6). Figure 6 shows that the particles have more clearly outlined contours at a heating temperature of 700 °C at all magnifications. Proceeding from this fact, it is possible to conclude that vanadium oxide phase on aluminum oxide surface is in weakly crystallized state up to melting temperature and after melting, when it is cooled down, it has more distinct crystalline structure. It should be noted that there is no significant change in particle size.

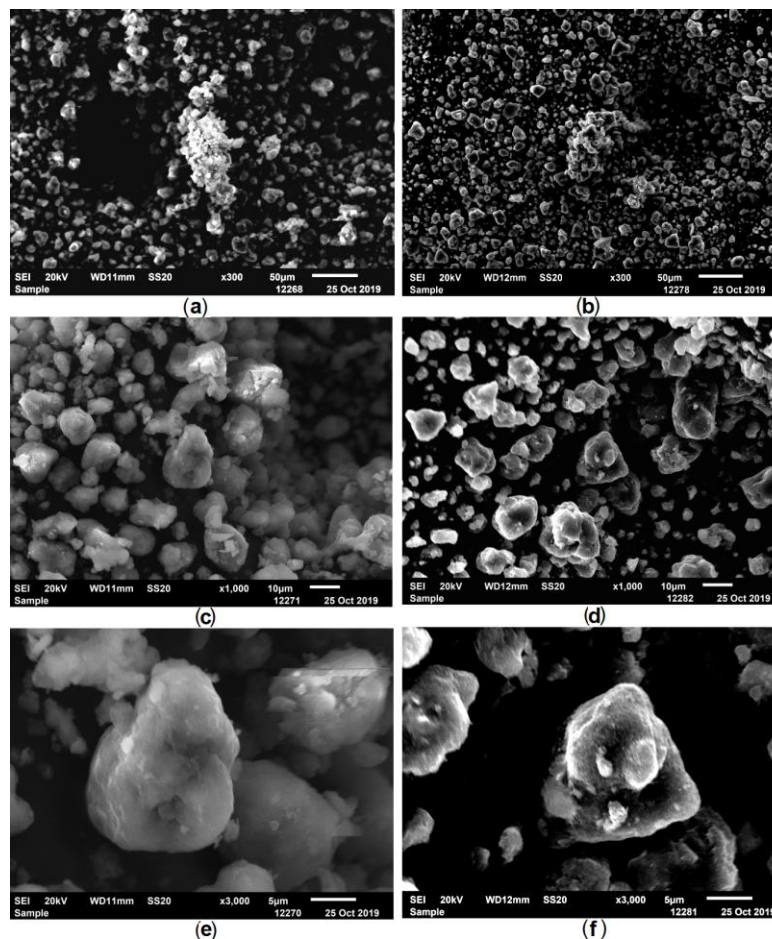


**Figure 6.** Micrographs of the 10% V/Al<sub>2</sub>O<sub>3</sub> system at different magnifications and heating temperatures: (a) - magnification by 300 times, 500 °C; (b) - magnification by 300 times, 700 °C; (c) - magnification by 1,000 times, 500 °C; (d) - magnification by 1,000 times, 700 °C; (e) - magnification by 3,000 times, 500 °C; (f) - magnification by 1,000 times, 700 °C.

The specific surface area (*S*) of samples of aluminium-vanadium phases at different temperatures were determined by the BET method by low-temperature nitrogen adsorption (Table 3). It follows from the obtained data that the surface of samples was in the region of 172 - 195 m<sup>2</sup>/g in the temperature range of 25 – 600 °C. Under literature data V<sub>2</sub>O<sub>5</sub> melts at 670-690 °C [39-40]. The surface of the catalyst decreased by about 6.5 times after the melting of vanadium oxides at 700 °C compared with the surface of sample heated at 600°C, from 174 to 27 m<sup>2</sup>/g. Aluminium oxide surface without vanadium oxide changes insignificantly from 195 to 189 m<sup>2</sup>/g in the same temperature range.

**Table 3.** Specific surface area of samples of aluminum-vanadium phases after calcination in air at different temperatures.

Sample	S (m <sup>2</sup> /g)
VOSO <sub>4</sub> ·3H <sub>2</sub> O vanadyl sulfate	23
10% V/γ-Al <sub>2</sub> O <sub>3</sub> from VOSO <sub>4</sub> ·3H <sub>2</sub> O, initial	192
10% V/γ-Al <sub>2</sub> O <sub>3</sub> from VOSO <sub>4</sub> ·3H <sub>2</sub> O, 1 h, 300 °C, air	184
10% V/γ-Al <sub>2</sub> O <sub>3</sub> from VOSO <sub>4</sub> ·3H <sub>2</sub> O, 1 h, 400 °C, air	195
10% V/γ-Al <sub>2</sub> O <sub>3</sub> from VOSO <sub>4</sub> ·3H <sub>2</sub> O, 1 h, 500 °C, air	172
10% V/γ-Al <sub>2</sub> O <sub>3</sub> from VOSO <sub>4</sub> ·3H <sub>2</sub> O, 1 h, 600 °C, air	174
10% V/γ-Al <sub>2</sub> O <sub>3</sub> from VOSO <sub>4</sub> ·3H <sub>2</sub> O, 1 h, 700 °C, air	27
10% V/γ-Al <sub>2</sub> O <sub>3</sub> from VOSO <sub>4</sub> ·3H <sub>2</sub> O, 1 h, 800 °C, air	10
γ-Al <sub>2</sub> O <sub>3</sub> after calcination in air at 600 °C, 1 h	195
γ-Al <sub>2</sub> O <sub>3</sub> after calcination in air at 700 °C, 1 h	189

It can be concluded that vanadium is preserved on the aluminium oxide surface even after the melting of V<sub>2</sub>O<sub>5</sub> oxide at temperatures above 600 °C. Moreover, its relative content increases as a result of the decomposition of aluminum and vanadium sulfates (Table 3).

The 10% V/γ-Al<sub>2</sub>O<sub>3</sub> system was reduced by the temperature-programmed reaction TPR-H<sub>2</sub> method by varying the preheating temperature in air. TPR-H<sub>2</sub> spectra are shown in Figure 7, their results are given in Table 4.

**Table 4.** Results of the 10% V/γ-Al<sub>2</sub>O<sub>3</sub> system study using TPR-H<sub>2</sub>.

Temperature of heating in air (°C)	Total area of peaks (a.u.)	Temperature of the peaks (°C)
25	14,407,832	640, 670
300	11,858,380	640, 670
400	11,382,953	640
500	11,110,654	650
600	11,063,026	635
700	7,920,939	645
800	8,052,778	645

As follows from Figure 7 and Table 4 two peaks at 640 and 670 °C are observed in the initial sample (25 °C). It can be assumed that they are associated with the interaction of hydrogen with oxygen of vanadium oxide and oxygen of vanadyl sulfate. Based on the EPR data (Table 1), the more intense peak at 640 °C belongs to vanadium oxide. The relatively high temperatures of the TPR peaks in our case, in contrast to the data [29] for vanadium-aluminium catalysts, may be due to the higher vanadium content in our case, as well as another initial vanadium compound used to prepare the catalyst.

The same situation is kept for 300 °C. At the same time, there is a decrease in the total area of the peaks (Table 4) due to a decrease in the amount of vanadyl sulfate.

Starting from 400 °C there is only one peak corresponding to oxygen of vanadium oxide in the spectra. It should be noted that the positions of the peaks and their area are almost the same in the range of 400 - 600 °C. It indicates the completion of the 10% V/γ-Al<sub>2</sub>O<sub>3</sub> catalytic system formation after 300 °C.

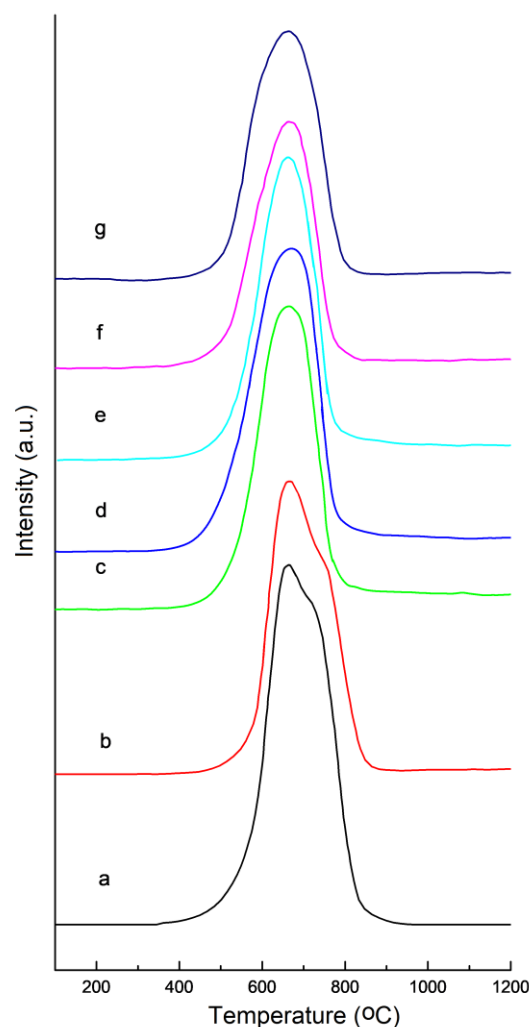
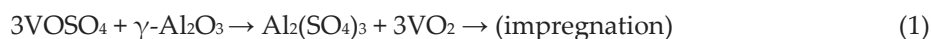


**Figure 7.** Reduction of the 10% V/ $\gamma$ -Al<sub>2</sub>O<sub>3</sub> system by TPR-H<sub>2</sub> method when varying the preheating temperature in air. (a) - 25 °C; (b) - 300 °C; (c) - 400 °C; (d) - 500 °C; (e) - 600 °C; (f) - 700 °C; (g) - 800 °C.

The decrease of the peak area at 700 °C and above is associated with the vanadium oxide melting (BET method, Table 3).

Thus, the data obtained in the study of physical and chemical properties of the 10% V/ $\gamma$ -Al<sub>2</sub>O<sub>3</sub> system in the process of its preparation enable to describe the processes occurring in this case according to the following scheme:



Therefore, the thermal decomposition of vanadyl sulfate should not lead to side effects (formation of additional phases), since this process results in the formation of the  $\gamma$ -Al<sub>2</sub>O<sub>3</sub> phase, which is similar to the initial carrier.

The S-curve data shown in Figure 8 was obtained from testing the activity of a vanadium-containing catalyst system.

The catalyst showed the lowest activity at a heating temperature of 300 °C (Figure 8, curve 1). Apparently, the presence of the product of the interaction between the carrier and vanadyl sulfate on the surface reduces its catalytic activity. The presence of strong interaction of vanadyl sulfate with aluminum oxide of the carrier is evidenced by the EPR data (Table 1). The catalyst activity increases (Figure 8, curve 4) and the sample itself from dark green at 300 °C (almost black) turns to orange color at 600 °C when the same

catalyst is reheated at 600 °C in air during 1 h in order to decompose this complex. It may indicate the presence of an inactive complex of vanadyl sulfate with aluminum oxide at 300 °C, and its destruction as the temperature increases with the formation of a more active complex with  $V_2O_5$ .

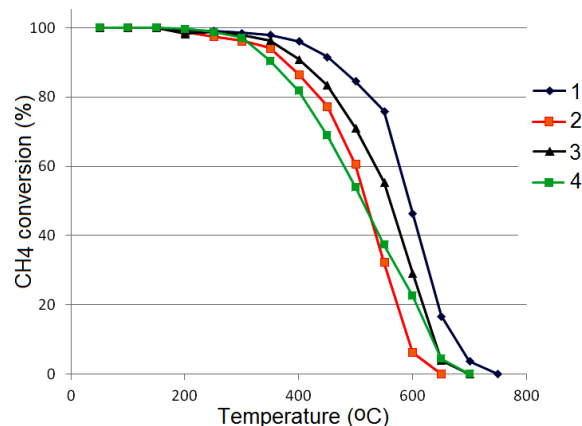


**Figure 8.** The relative content of methane in the methane-air mixture after the reaction on the 10% V/Al<sub>2</sub>O<sub>3</sub> catalyst at different temperatures: 1 - heating of the catalyst in air for 1 h at 300 °C; 2 - at 600 °C for 1 h; 3 - at 700 °C for 1 h; 4 - sample additionally heated at 600 °C for 1 h after all measurements.

As shown above, the specific surface area of the catalyst sharply decreases from 174 to 27 m<sup>2</sup>/g, (Table 3). This is due to the melting of vanadium oxide with an increase in the heating temperature from 600 to 700 °C. The catalyst activity in methane oxidation at these temperatures was determined. The data are shown in Figure 8, Curves 2, 3. Activity of the catalyst heated at 700 °C is somewhat lower than activity of the catalyst heated at 600 °C. In spite of the fact that specific surface decreases more than in 6 times in this case, catalyst activity decreases not so significantly, and its activity is higher than catalyst activity warmed up at 300 °C (Figure 8, Curves 3, 4).

### 3. Materials and Methods

The catalytically active phase was prepared by impregnating the  $\gamma$ -Al<sub>2</sub>O<sub>3</sub> carrier with an aqueous solution of vanadyl sulfate followed by heat treatment. Vanadyl sulfate was chosen as initial compound due to the possibility to obtain aqueous solutions of high concentration and low decomposition temperature (lower than the melting point of vanadium (V) oxide).

The dependence of the catalytic properties of the vanadium-containing phase on the preheating temperature in air was evaluated. For this purpose, 10% V/Al<sub>2</sub>O<sub>3</sub> catalysts (per metallic vanadium) were prepared on metallic blocks (neutralizer body) from X15U5 Fechral.

The simplest hydrocarbon methane was used to simulate the interaction of the saturated hydrocarbons with the neutralizers.

Activity tests were performed in a flow-through apparatus at atmospheric pressure with chromatographic control of methane concentration in the gas mixture (1% methane in argon - air) before and after the catalyst. The ratio of methane to oxygen in the mixture before reaction was 1/15 at space velocity of 25,000 h<sup>-1</sup>. The initial catalyst with a secondary carrier from alumina was preliminarily impregnated with an aqueous salt solution of VOSO<sub>4</sub>·3H<sub>2</sub>O according to its moisture capacity and dried at room temperature. Then the catalyst was heated in air at a given temperature for 1 h and placed in a quartz reactor. Methane content before and after passage through the catalyst was measured at different temperatures of the gas mixture (methane-argon-air) on a gas chromatograph with a flame ionization detector.

Electron paramagnetic resonance (EPR) studies were performed at room temperature with a JES ME ESR spectrometer, JEOL, in the 3-cm range.

A surface analyzer, AccuSorb gas adsorption porosimeter, Micromeritics, was used in the BET method for low-temperature nitrogen adsorption.

Microphotographs were taken with a JSM 6610 LV scanning electron microscope, JEOL, at different magnifications. The accelerating voltage was 20 kV, imaging mode was SEL.

The elemental composition was determined using an INCA Energy 450 energy dispersive microanalysis system mounted on a JSM 6610 LV scanning electron microscope, JEOL.

X-ray diffractometry was performed on DRON-4M X-ray diffractometer. A tube with a cobalt cathode was used. Imaging conditions were tube voltage 30 kV, current 20 mA; sweep rate 2 °/min.

Thermo-programmed hydrogen reduction (TPR-H<sub>2</sub>) of the 10% V/γ-Al<sub>2</sub>O<sub>3</sub> system was performed between 25 and 1,100 °C in linear mode with the 5% mixture of hydrogen and argon at a temperature change rate of 5 °C/min. The gas flow rate was 30 ml/min. Signals were recorded using a thermal conductivity detector on the Crystal 5000 "Chromatec" chromatograph.

#### 4. Conclusions

As a result of this research it was possible to show that the catalytically active vanadium-containing system includes several complexes with different thermal stability and catalytic activity. The presence of thermal stable, but inactive spinel complexes with aluminium oxide, which are quite easily formed from low-valent s- and d-elements and aluminum oxide, was not detected in the system at moderate heating [22, 37].

As the temperature of heat treatment increases, the low-active vanadyl sulfate complexes decompose with the formation of more active ones based on V<sub>2</sub>O<sub>5</sub> oxide. It can be assumed that V<sub>2</sub>O<sub>5</sub> oxide plays the determining role in the catalytic activity of the system.

Thus, the 10% V/Al<sub>2</sub>O<sub>3</sub> system in the studied temperature range is thermal stable and exhibits high activity not only in the reduction of nitrogen oxides [31-37] but also in the oxidation of hydrocarbons (even the most difficult oxidizable methane). These properties of the system make it quite promising in the field of application for purification of exhaust gases of motor vehicles and industrial enterprises from environmentally harmful components as well as for understanding the mechanism of the action of catalysts in these processes, which is very important for solving the problems of decarbonization and achieving carbon neutrality.

**Author Contributions:** Conceptualization, B.Kh. and A.S.; methodology, A.S. and A.B.; validation, K.R.; formal analysis, V.Y., V.G., A.I., A.Sh., I.Sh.; investigation, K.R., A.S., A.B.; writing—original draft preparation, A.B., A.S.; writing—review and editing, A.B., A.S.; visualization, A.I., A.Kh; supervision, A.S., B.Kh., A.B., S.T. All authors have read and agreed to the published version of the manuscript.

**Funding:** This research was funded by Science Committee of the Ministry of Education and Science of the Republic of Kazakhstan, grant number AP08856680.

**Data Availability Statement:** The data presented in this study are available upon request from the corresponding author

**Acknowledgments:** The authors are especially grateful to Academician M. Zhurinov from the National Academy of Sciences of the Republic of Kazakhstan for his support in the research under this work.

**Conflicts of Interest:** The authors declare no conflict of interest. The funders had no role in the design of the study; in the collection, analyses, or interpretation of data; in the writing of the manuscript; or in the decision to publish the results.

## References

1. Garbowski, E.; Guenin, M.; Marion, M.; Primet, M. Catalytic properties and surface states of cobalt-containing oxidation catalysts. *Appl. Catal.* **1990**, *64*, 209-224.
2. Zeng, H.; Ji, L.; Lin, J. Metal-support interactions in Co/Al<sub>2</sub>O<sub>3</sub> catalysts. A comparative study on reactivity of support. *Phys. Chem.* **2000**, *104*, 1783-1790.
3. Thormählen, P.; Skoglundh, M.; Fridell, E.; Andersson, B. Low-temperature CO oxidation over platinum and cobalt oxide catalysts. *J. Catal.* **1999**, *188*, 300-310.
4. Avgouropoulos, G.; Ioannides, T.; Papadopoulou, C.; Batista, J.; Hocevar, S.; Matralis, H.K. A Comparative study of Pt/ $\gamma$ -Al<sub>2</sub>O<sub>3</sub>, Au/ $\alpha$ -Fe<sub>2</sub>O<sub>3</sub> and CuO-CeO<sub>2</sub> catalysts for the selective oxidation of carbon monoxide in excess hydrogen. *Catal. Today* **2002**, *75*, 157-167.
5. Jansson, J. Low-temperature CO oxidation over Co<sub>3</sub>O<sub>4</sub>/Al<sub>2</sub>O<sub>3</sub>. *J. Catal.* **2000**, *194*, 55-60.
6. Ma, W.; Jacobs, G.; Keogh, R.A.; Bukur D.B.; Davis, B.H. Fischer-Tropsch synthesis: Effect of Pd, Pt, Re, and Ru noble metal promoters on the activity and selectivity of a 25% Co/Al<sub>2</sub>O<sub>3</sub> catalyst. *Appl. Catal. A Gen* **2012**, *437*, 1-9.
7. Rattan, G.; Kumar, M. Carbon monoxide oxidation using cobalt catalysts. *Chem. Chem. Technol.* **2014**, *8*, 249-260.
8. Zavyalova, U.F.; Tretyakov, V.F.; Burdeinaya, T.N.; Lunin, V.V.; Titkov, A.I.; Salanov, A.N.; Ryzhova, N.D.; Tsyrylnikov, P.G. Oxidation of CO, deep oxidation of CH<sub>4</sub> and reduction of NO<sub>x</sub> by propane on CuCo<sub>2</sub>O<sub>4</sub> and Pd-CeO<sub>2</sub> catalysts supported on tape carriers. *Pet. Chem.* **2005**, *45*, 281-286. (in Rus.).
9. Zavyalova, U.F.; Petrov, V.F.; Burdeinaya, T.N.; Tsyrylnikov, T.N. Block catalysts for neutralization of exhaust gases synthesized by the combustion method. *Chemistry for Sustainable Development* **2005**, *13*, 751 - 755. (in Rus.).
10. Noskov, A.S.; Pai, Z.P. *Technological methods for protecting the atmosphere from harmful emissions at energy enterprises*, SB RAS: Novosibirsk, Russia, 1996; p. 156. (in Rus.).
11. Popova, N.M. *Catalysts for the purification of gas emissions from industrial production*, Nauka: Alma-Ata, Kazakh SSR, 1991; p. 176. (in Rus.).
12. Borshch, V.N.; Pugacheva, E.V.; Zhuk, S.Ya.; Andreev, D.E.; Sanin, V.N.; Yukhvid, V.I. Multicomponent metal catalysts for deep oxidation of carbon monoxide and hydrocarbons. *Proceedings of the Academy of Sciences* **2008**, *419*, 775-777. (in Rus.).
13. Vaneman, G. L. Comparison of metal foil and ceramic monolith automotive catalytic converters. *Catalysis and automotive pollution control II*. **1991**, *71*, 537 - 555.
14. Anders, J.J.; Palmqvist, E.C.; Fridell, E.; Skoglundh, M.; Österlund, L.; Thormählen, P.; Langer, V. On the catalytic activity of Co<sub>3</sub>O<sub>4</sub> in low-temperature CO oxidation. *J. Catal.* **2002**, *211*, 387-397.
15. Wang, H.F.; Kavanagh, R.; Guo, Y.L.; Guo, Y.; Hu, P. Synthesis-structure-activity relationships in Co<sub>3</sub>O<sub>4</sub> catalyzed CO oxidation. *J. Catal.* **2012**, *296*, 110-119.
16. Ozkara, S.; Akin, A.N.; Misirli, Z.; Aksoylu, A.E. The effect of metal loading on structural characteristics and low temperature CO oxidation activity of coprecipitated Co/Al<sub>2</sub>O<sub>3</sub>. *Turk. J. Chem.* **2005**, *29*, 219-224.
17. Oliveira, H.A.; Franceschini, D.F.; Passos, F.B. Cobalt catalyst characterization for methane decomposition and carbon nanotube growth. *Journal of the Brazilian Chemical Society*. **2014**, *25*, 53-65.
18. Vosoughi, V.; Dalai, A.K.; Abatzoglou, N.; Hu, Y. Performances of promoted cobalt catalysts supported on mesoporous alumina for Fischer-Tropsch synthesis. *Appl. Catal. A Gen* **2017**, *547*, 155-163.
19. Kurzina I.A. Deep oxidation of methane on platinum and palladium catalysts supported on silicon nitride. *Bulletin of the Tomsk Polytechnic University* **2005**, *308*, 104 -109.
20. Ivanova, N.D.; Ivanov, S.V.; Boldyrev, E.I.; Sokolsky, G.V.; Makeeva, I.S. Highly efficient manganese oxide catalysts for the CO oxidation reaction. *Journal of Applied Chemistry* **2002**, *75*, 1452-1455.
21. Olsson, L.; Fridell, H.; Skoglundh, M.; Andersson, B. A kinetic study of NO oxidation and NO<sub>x</sub> storage on Pt/Al<sub>2</sub>O<sub>3</sub> and Pt/BaO/Al<sub>2</sub>O<sub>3</sub>. *J. Phys. Chem. B* **2001**, *105*, 6895-6906.
22. Massenova, A.; Kalykberdiyev, M.; Ussenov, A.; Sass, A.; Kenzin, N.; Kanatbayev, E.; Baiken, A. Catalytic technologies for the production of eco-friendly gasolines and reducing the toxicity of vehicle exhaust gases. *Oriental Journal of Chemistry* **2019**, *35*, 351-357.
23. Gruber, M.; Hermann, K. Elementary steps of the catalytic NO<sub>x</sub> reduction with NH<sub>3</sub>: Cluster studies on reaction paths and energetics at vanadium oxide substrate. *J. Chem. Phys.* **2013**, *139*, 244701-244708.
24. Kalinkin, P.; Kovalenko, O.; Lapina, O.; Khabibulin, D.; Kundo, N. Kinetic peculiarities in the low-temperature oxidation of H<sub>2</sub>S over vanadium catalysts. *J. Mol. Catal. A Chem.* **2002**, *178*, 173-180.
25. León, M.; Jiménez-Jiménez, J.; Jiménez-López, A.; Rodríguez-Castellón, E.; Soriano, D.; Nieto, J.M.L. Vanadium oxide-porous phosphate heterostructure catalysts for the selective oxidation of H<sub>2</sub>S to sulphur. *Solid State Sci.* **2010**, *12*, 996-1001.
26. Barba, D.; Palma, V.; Ciambelli, P. Screening of catalysts for H<sub>2</sub>S abatement from biogas to feed molten carbonate fuel cell. *Int. J. Hydrogen Energy* **2013**, *38*, 328-335.
27. Soriano, M.D.; Nieto, J.M.L.; Ivars, F.; Concepcion, P.; Rodriguez-Castellon, E. Alkali-promoted V<sub>2</sub>O<sub>5</sub> catalysts for the partial oxidation of H<sub>2</sub>S to sulphur. *Catal. Today* **2012**, *192*, 28-35.
28. Amiridis, M. D.; Solar, J. P. Selective catalytic reduction of nitric oxide by ammonia over V<sub>2</sub>O<sub>5</sub>/TiO<sub>2</sub>, V<sub>2</sub>O<sub>5</sub>/TiO<sub>2</sub>/SiO<sub>2</sub>, and V<sub>2</sub>O<sub>5</sub>-WO<sub>3</sub>/TiO<sub>2</sub> catalysts: Effect of vanadia content on the activation energy. *Ind. Eng. Chem. Res.* **1996**, *35*, 978-981.
29. Garbarino, G.; Kowalik, P.; Riani, P.; Antoniuk-Jurak, K.; Pieta, P.; Lewalska-Graczyk, A.; Lisowski, W.; Nowakowski, R.; Busca, G.; Pieta, I. Improvement of Ni/Al<sub>2</sub>O<sub>3</sub> catalysts for low-temperature CO<sub>2</sub> methanation by vanadium and calcium oxide addition. *Ind. Eng. Chem. Res.* **2021**, *60*, 6554-6564.

30. Wachs, I.E. Catalysis science of supported vanadium oxide catalysts. *Dalton Trans.* **2013**, *42*, 11762-11769.
31. Koebel, M.; Elsener, M.; Kleemann, M. Urea-SCR: a promising technique to reduce NO<sub>x</sub> emissions from automotive diesel engines. *Catal. Today* **2000**, *59*, 335-345.
32. Forzatti, P. Present status and perspectives in de-NO<sub>x</sub> SCR catalysis. *Appl. Catal. A Gen* **2001**, *222*, 221-236.
33. Borovkov, V.Yu.; Mikheeva, E.P.; Zhidomirov, G.M.; Lapina, O.B. Theoretical and experimental studies of the nature of the catalytic activity of VO<sub>x</sub>/TiO<sub>2</sub> systems. *Kinet. Catal.* **2003**, *44*, 710-717.
34. Wu, M.; Ung, K.C.; Dai, Q.; Wang, X. Catalytic combustion of chlorinated VOCs over VO<sub>x</sub>/TiO<sub>2</sub> catalysts. *Catal. Commun.* **2012**, *18*, 72-75.
35. Inomata, Y.; Hata, Sh.; Mino, M.; Kiyonaga, E.; Morita, K.; Hikino, K.; Yoshida, K.; Kubota, H.; Toyao, T.; Shimizu, K.; Haruta, M.; Murayama, T. Bulk vanadium oxide versus conventional V<sub>2</sub>O<sub>5</sub>/TiO<sub>2</sub>: NH<sub>3</sub>-SCR catalysts working at a low temperature below 150 °C. *Amer. Chem. Soc. Catal.* **2019**, *9*, 9327-9331.
36. Marberger, A.; Elsener, M.; Ferri, D.; Kröcher, O. VO<sub>x</sub> surface coverage optimization of V<sub>2</sub>O<sub>5</sub>/WO<sub>3</sub>-TiO<sub>2</sub> SCR catalysts by variation of the V loading and by aging. *Catalysts.* **2015**, *5*, 1704-1720.
37. Massenova, A.; Kalykberdiyev, M.; Sass, A.; Kenzin, N.; Ussenov, A.; Baiken, A.; Rakhmetova, K. Catalytic technologies for solving environmental problems in the production of fuels and motor transport in Kazakhstan. *Catalysts* **2020**, *10*, 1-21.
38. Rovenskikh, A.S.; Kariychina, A.E.; Iguminova, V.A. Automobile emission effect on the environment. Investigations of young scientists. In Proceedings of the XV International scientific conference, Kazan, Russia, 24 December 2020, p. 15-18. (in Rus.).
39. Zeidel, A.N.; Prokofiev, V.K.; Raysky, S.M.; Slavny, V.A.; Schrader, E.Ya. *Tables of spectral lines. Directory*, Nauka: Moscow, Russia, 1977; p. 800. (in Rus.).
40. Kalinkin, I.P.; Mosichev V.I. *New handbook of chemist and technologist. Analytical chemistry*, Peace and Family: St. Petersburg, Russia, 2003; p. 984. (in Rus.).